Photoneutron Cross Sections of Tb^{159} and O^{16}†

R. L. Bramblett, J. T. Caldwell, R. R. Harvey, and S. C. Fultz
Lawrence Radiation Laboratory, University of California, Livermore, California
(Received 7 October 1963)

The photoneutron cross sections of O^{16} and Tb^{159} have been measured up to 30 MeV using photons of 3% resolution resulting from positron annihilation-in-flight. Thirteen resonances corresponding to levels in O^{16} were observed in the $O^{16}(\gamma,n)$ reaction. One, at 29±1 MeV, is previously unreported. The $O^{16}(\gamma,n)$ cross section integrated to 30 MeV is 46±5 MeV-mb. Both the (γ,n) and $(\gamma,2n)$ cross sections of Tb were measured using a statistical counting technique. The ratio of the two cross sections determines that the level density parameter, $a=17\pm5$ $(\text{MeV})^{-1}$. The sum of the (γ,n) and $(\gamma,2n)$ cross sections is a double peaked giant $E1$ resonance, from which the intrinsic quadrupole moment was determined to be 7.0±1.1 b. Additional structure in the $Tb^{159}(\gamma,n)$ cross section was observed at 10.1 MeV. The sum of the (γ,n) and $(\gamma,2n)$ cross sections of Tb^{159}, integrated to 28 MeV, is 2.3±0.2 MeV-b.

I. INTRODUCTION

A RECENTLY developed technique[1–4] for producing monoenergetic photons has been used to measure the photoneutron cross sections of Tb^{159} and O^{16} from threshold to 30 MeV. The technique does not involve an unfolding process, as is required for measurements which use bremsstrahlung. Thus, it enables better absolute cross section determinations at higher photon energies. In addition, a technique for measuring the $(\gamma,2n)$ cross section simultaneously with the (γ,n) cross section has been used. Consequently, it is not necessary to apply a calculated correction to the neutron yield to account for the $(\gamma,2n)$ contribution.

The Tb and O cross sections are quite different, since Tb^{159} is highly deformed and has many closely spaced levels which form a double giant electric dipole resonance for photon absorption, and O^{16} has widely spaced levels which result in resolvable resonances. Hence, the description of both cross sections is a severe test of any photonuclear theory. The shell model with accounts for particle-hole interactions does seem to be near such a description. The electric dipole photon absorption in O^{16} has been calculated in detail on the basis of the shell model.[5–8] Detailed calculations for heavy nuclei such as Tb^{159} have not been performed, although simplified calculations by Wilkinson[9] and Brown[10] indicate that the photon interaction for heavy nuclei can be described using the shell model.

In the absence of detailed calculations for Tb^{159}, which are very laborious, the semiclassical hydrodynamic model[11,12] for photon absorption has been used to determine the nuclear deformation of Tb from the cross section. The hydrodynamic model was the first to predict the splitting of the giant $E1$ resonance into two components, and has been quite successful in predicting the shape of the resonance.[2–4]

II. EXPERIMENTAL TECHNIQUE

Monoenergetic photons were obtained by annihilation-in-flight of monoenergetic positrons. The apparatus is shown in Fig. 1. The positrons were produced at the end of the first section of a two-stage linear accelerator by 10-MeV electrons which bombarded a 0.1-in.-thick W target. The second accelerator section was used to accelerate the positrons to the desired energy, which ranged from 8 to 28 MeV. The positrons were magnetically analyzed with 1% resolution and focused on a 0.060-in.-thick LiH target, where some annihilated in flight. Positrons that penetrated the target were swept out of the photon beam by a strong magnet. At 0° to the positron direction the photon energy is equal to the positron energy plus about 0.76 MeV, and the photon energy resolution was about 3%, due to scattering in the LiH target. The photon intensity was monitored by a xenon transmission ion chamber which had been calibrated using a 5-×6-in. NaI spectrometer. The sample was positioned axially in a 4π, BF_3-paraffin, neutron detector which had about 20% detection efficiency. The oxygen sample was 150 g of H_2O and the terbium sample was 320 g of Tb_4O_7. A very small correction was applied to the Tb_4O_7 data to account for the $O^{16}(\gamma,n)$ reaction.

A typical photon spectrum as recorded by the NaI spectrometer is shown in Fig. 2. In addition to the annihilation photon peak, the figure also shows the bremsstrahlung produced by positrons. The effect of this positron bremsstrahlung was removed by taking

† Work done under the auspices of the U. S. Atomic Energy Commission.

[1] C. R. Hatcher, R. L. Bramblett, N. E. Hansen, and S. C. Fultz, Nucl. Instr. Methods **14**, 337 (1961).
[2] S. C. Fultz, R. L. Bramblett, J. T. Caldwell, and N. A. Kerr, Phys. Rev. **127**, 1273 (1962).
[3] S. C. Fultz, R. L. Bramblett, J. T. Caldwell, N. E. Hansen, and C. P. Jupiter, Phys. Rev. **128**, 2345 (1962).
[4] R. L. Bramblett, J. T. Caldwell, G. F. Auchampaugh, and S. C. Fultz, Phys. Rev. **129**, 2723 (1963).
[5] J. P. Elliott and B. H. Flowers, Proc. Roy. Soc. (London) **A242**, 57 (1957).
[6] G. E. Brown, L. Castillejo, and J. A. Evans, Nucl. Phys. **22**, 1 (1960).
[7] V. Gillet and N. Vinh Mau, Phys. Letters **1**, 25 (1962).
[8] J. Sawicki and T. Soda, Nucl. Phys. **28**, 270 (1961).
[9] D. H. Wilkinson, Phil. Mag. **3**, 567 (1958).
[10] G. E. Brown and M. Bolsterli, Phys. Rev. Letters **3**, 472 (1959).
[11] H. Steinwedel and J. H. D. Jensen, Z. Naturforsch. **5a**, 413 (1950).
[12] M. Danos, Nucl. Phys. **5**, 23 (1956).

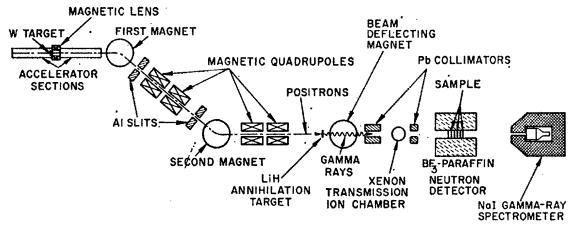

FIG. 1. Experimental apparatus for photoneutron cross section measurements. The drawing is not to scale. Neutron shields and some gamma-ray shielding have been omitted.

neutron counts using both positrons and electrons to bombard the LiH target, and subtracting the results. The pulsed nature of the linear accelerator and the small number of reactions per accelerator pulse facilitated the measurement of the $(\gamma,2n)$ cross section of Tb^{159}. The number of accelerator pulses for which one, two, or three neutrons were detected was recorded, and a statistical analysis was used to determine the $(\gamma,2n)$ cross section. More details of the experimental technique are contained in previous reports.[1–4]

III. $O^{16}(\gamma,n)O^{15}$

The (γ,n) cross section obtained for O^{16} is shown in Fig. 3. The 13 resonances observed in this experiment are marked by short arrows. The widths of the peaks are all about the same as the experimental resolution, so it is possible that some of them are narrow; thus the cross sections at the peaks are not meaningful. However, the integrated cross sections can be compared with those obtained by other techniques and with relative transition strengths predicted by theory. The $O^{16}(\gamma,n)$ cross section of Fig. 3 integrated to 24 MeV is 23 ± 2 MeV-mb. This integrated cross section is in good agreement with that obtained using bremsstrahlung. For example, Roalsvig, Gupta, and Haslam[13] averaged seven bremsstrahlung determinations previous to 1958 and obtained, up to 24 MeV, an integrated cross section of 26 ± 3 MeV-mb. Our integrated cross section is also in agreement with the recent bremsstrahlung measurements of Bolen and Whitehead,[14] and with Miller, Schuhl, Tamas, and Tzara,[15] who used an annihilation photon technique. The $O^{16}(\gamma,p)$ cross section, integrated to 27 MeV, has been determined by Dodge and Barber.[16] Assuming 100% ground-state transitions, it is 56 ± 11 MeV-mb. The (γ,n) cross section of Fig. 3 integrated to 27 MeV is 37 ± 4 MeV-mb, thus the ratio of the (γ,n) to (γ,p) cross sections for oxygen is 0.7 ± 0.2, in fair agreement with the ratio 1 predicted by charge independence of nuclear forces.[17] The sum of the (γ,n) and (γ,p) cross sections integrated to 27 MeV is 93 MeV-mb, which is less than half of the Thomas-Reiche-Kuhn sum rule, 60 NZ/A MeV-mb, for $E1$ photon absorption.

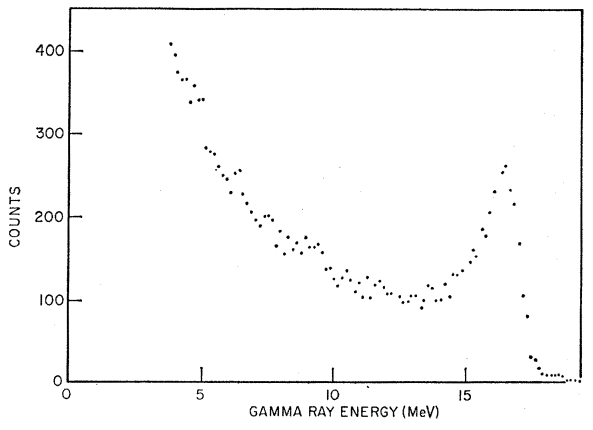

FIG. 2. NaI pulse-height spectrum of gamma rays from 15.6-MeV positrons incident on a 0.060-in.-thick LiH target.

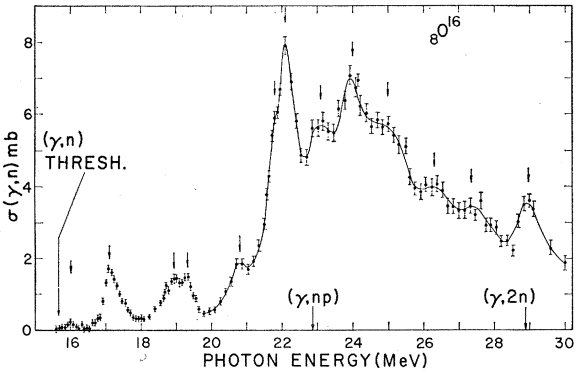

FIG. 3. Photoneutron cross section of O^{16} up to 30 MeV, showing resonances due to levels in O^{16}. The shell model predicts four electric dipole transitions in this energy range.

Using the neutron multiplicity counting technique described previously,[2–4] an attempt was made to measure the $O^{16}(\gamma,2n)$ cross section above the threshold at 28.9 MeV.[18] No neutrons due to $(\gamma,2n)$ reactions were observed. The data indicate that the $(\gamma,2n)$ cross section is less than 0.1 mb up to 29.9 MeV.

The energy levels in O^{16} observed in this experiment are compared with those obtained in other experiments in Table I. We estimate our energy calibration to be good to 1%; the calibration of the other experiments should be better than 1%. Column 1 contains our results. Firk and Lokan[19] used bremsstrahlung and measured the neutron energies from the $O^{16}(\gamma,n)O^{15}$ reaction, using time-of-flight techniques. They identified the structure in the neutron spectrum due to levels in

[13] J. P. Roalsvig, I. C. Gupta, and R. N. H. Haslam, Can. J. Phys. **39**, 643 (1961).

[14] L. N. Bolen and W. D. Whitehead, Phys. Rev. Letters **9**, 458 (1962).

[15] J. Miller, C. Schuhl, G. Tamas, and C. Tzara, Phys. Letters **2**, 76 (1962), corrected in internal report.

[16] W. R. Dodge and W. C. Barber, Phys. Rev. **127**, 1746 (1962).

[17] F. C. Barker and A. K. Mann, Phil. Mag. **2**, 5 (1957).

[18] *Nuclear Data Sheets*, compiled by K. Way *et al.* (Printing and Publishing Office, National Academy of Science–National Research Council, Washington 25, D. C.).

[19] F. W. K. Firk and K. H. Lokan, Phys. Rev. Letters **8**, 321 (1962).

TABLE I. Energy levels observed for O^{16}.

$O^{16}(\gamma,n)4\pi$ (MeV) Present work	$O^{16}(\gamma,n)70°$ (MeV)[a]	$N^{15}(p,\gamma)$ (MeV)[b]	$O^{16}(e,p)76°$ (MeV)[c]
16.0		16.2(1+)	
		17.2(1−)	
17.1		17.3(1−)	17.3
19.0	19.1	19.0	19.0
19.3	19.6	19.5	19.6
20.8	20.7	20.8	20.6
	21.0		
21.8	21.7		
22.1	22.2	22.3	22.3
23.1	23.0	23.1	23.1
24.0	24.3	24.4	24.4
25.0	25.0	25.0	
	~25.4		
26.2	26.3		
27.3			
28.9			

[a] See Ref. 19.
[b] See Ref. 20.
[c] See Ref. 16.

O^{16}; their results are in Column 2. Tanner, Thomas, and Earle[20] observed the ground-state gamma ray from $N^{15}(p,\gamma)O^{16}$ to determine the levels given in column 3. Dodge and Barber[16] used high-energy electrons and measured the proton energies from $O^{16}(e,p)N^{15}$ in a magnetic spectrometer (see column 4 of Table I). The four experiments are in excellent agreement. We observe two levels above 25 MeV that have not been observed using gamma rays. The 27-MeV level has been observed by Weil and Din[21] using the $C^{13}(He^3,n)O^{15}$ reaction.

The several shell-model calculations[5–8] of the $E1$ transition energies and strengths in O^{16} give essentially the same results. The calculations consider single-particle transitions from the $1p$ shell to the $2s$ and $1d$ shells. The transition energies are determined to first order from levels in mass 16 and 17 nuclei, and are perturbed by the residual interaction of the particle and the hole corresponding to the initial state of the particle. The experimental results are compared with the calculations of Elliott and Flowers[5] in Table II. Four transitions are predicted above the (γ,n) threshold, and resonances in the cross section are observed corresponding to each transition to within 5% in energy. In addition, several resonances are observed which are not predicted by the theory for $E1$ transitions. One of these, at 16 MeV, has been shown to be an $M1$ transition by Tanner, Thomas, and Earle.[20] The strengths of the transitions at 19, 23, 24, and 29 MeV are comparable with those of $E1$ transitions, and are in need of theoretical explanation. Particle-hole calculations by Gillet and Vinh Mau[7] predict the positions of several levels other than 1− levels in the region below 30 MeV. For example, a strong 2− level is predicted at 20 MeV which might be identified with the experimentally observed levels at 20.7 and 21.0 MeV; the 19.0-, 19.3-MeV state would then be a 1− state. However, detailed comparison of theory and experiment is premature for two reasons: (1) The theory does not predict the relative strengths of $E1$, $E2$, $M1$, and $M2$ transitions, and (2) the experiments do not determine the multipolarity of the transitions. The strengths of the first few transitions relative to the (γ,n) cross section integrated to 30 MeV are compared with the calculations of Elliott and Flowers[5] in Table II. The agreement is only qualitative; for example, the theoretical transition strength for the 22-MeV level is too large by a factor of 3, but it does appear to be the strongest transition, as predicted by theory.

TABLE II. Experimental and theoretical dipole strengths for O^{16}.

Experimental levels (MeV)	Particle-hole levels[a] (MeV)	Fractional strength[b] (experimental)	Fractional dipole strength[a] (theoretical)
16.0		0.002±0.001	
17.2	17.3	0.024±0.002	0.01
17.3			
19.0		0.04 ±0.01	
19.3			
20.7	20.4	0.05 ±0.02	0.001
21.0			
21.8	22.6	0.19 ±0.07	0.67
22.1			
23.1			
24.0			
25.0	25.2	0.5	0.32
25.4			
26.2			
27.3			
28.9		0.16 ±0.08	

[a] See Ref. 5.
[b] The $O^{16}(\gamma,n)$ cross section, integrated to 30 MeV, is 46±5 MeV-mb.

The widths of the resonances at 22 and 25 MeV have been calculated by Bauer[22] using the particle-hole shell model. The widths arise from the overlap of virtual state wave functions and continuum wave functions which consist of a core and a neutron or proton. Bauer obtained widths of 1.8 and 2.4 MeV for the 22- and 25-MeV levels. Our measurements indicate that the width of the 22 MeV-level is $\leq$0.7 MeV, and, again, the agreement of theory with experiment is only qualitative.

IV. $Tb^{159}(\gamma,n)$ AND $Tb^{159}(\gamma,2n)$

The $Tb^{159}(\gamma,n$ and $Tb^{159}(\gamma,2n)$ cross sections were determined from the neutron yield using the multiplicity counting technique described earlier; the resulting cross sections are shown in Fig. 4. The (γ,n) threshold has been determined by Geller, Muirhead, and Halpern[23] who obtained 8.14±0.04 MeV and Chidley, Katz, and

[20] N. W. Tanner, G. C. Thomas, and E. D. Earle, *Proceedings of the Rutherford Jubilee International Conference*, edited by J. E. Birks (Heywood and Company Ltd., Manchester, England, 1962).
[21] J. L. Weil and G. U. Din, Bull. Am. Phys. Soc. 7, 111 (1962).
[22] M. Bauer, thesis, University of Maryland, 1962 (unpublished).
[23] K. N. Geller, J. Halpern, and E. G. Muirhead, Phys. Rev. 118, 1302 (1960).

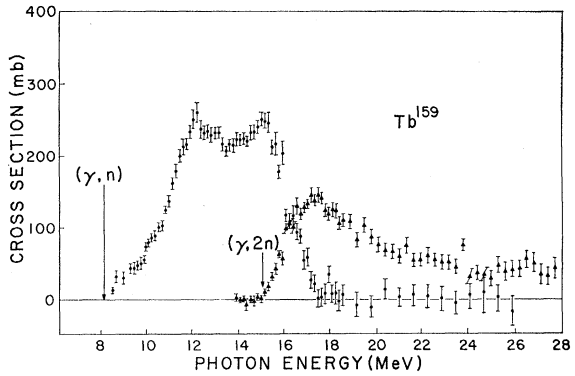

FIG. 4. The (γ,n) and $(\gamma,2n)$ cross sections of Tb^{159} up to 28 MeV. The (γ,n) cross section decreases rapidly to zero above the $(\gamma,2n)$ threshold.

Kowalski[24] who obtained 8.16±0.05 MeV. The observed $(\gamma,2n)$ threshold of 15.1±0.3 MeV is the first experimental determination of the mass Tb^{157}. Levy's empirical mass equation[25] yields 7.8 and 14.4 for the (γ,n) and $(\gamma,2n)$ thresholds.

The ratio of the (γ,n) and $(\gamma,2n)$ cross sections can be used to determine the nuclear level density parameter a for Tb^{158} if the spin dependence of the level density is neglected. Assuming that the nuclear level density is of the form $W(E) \propto \exp(2a^{1/2}E^{1/2})$ and neglecting the energy dependence of σ_c, the inverse cross section, our ratio of the $(\gamma,2n)$ cross section to the (γ,n) cross section is adequately described by the statistical model[26] with $a=15\pm3$ $(\text{MeV})^{-1}$. According to Ericson,[27] a more appropriate level density expression for a degenerate Fermi gas is $W(E) \propto E^{-2}\exp(2a^{1/2}E^{1/2})$. Using this form for the level density, $a=19\pm3$ $(\text{MeV})^{-1}$. Since Tb^{158} is an odd-odd nucleus, the pairing correction is zero.[28] The values of a obtained with either form for the level density are in approximate agreement with $A/10$ $(\text{MeV})^{-1}$ which is obtained in other experiments.[27]

The total photon absorption cross section of heavy nuclei above the neutron threshold is the sum of the neutron producing cross sections, since charged particle emission is negligible.[29] Figure 5 shows the sum of the (γ,n) and $(\gamma,2n)$ cross sections of Tb^{159}. The giant $E1$ resonance shows pronounced structure due to the large quadrupole moment of Tb^{159}. Wilkinson,[9] using the Nilsson shell-model levels for deformed nuclei, has considered the possible $E1$ transitions and calculated their strengths to obtain the shape of the giant resonance for deformed and closed-shell nuclei. The energy scale is undetermined, but the calculated giant resonance is split into two components, in agreement with the experiment. Wilkinson's calculation for $A=165$, $\delta=0.3$ is shown as the dashed curve in Fig. 5; it is normalized in energy and cross section at 12.2 MeV. Brown and Bolsterli[10] have shown how the energy scale of the shell-model calculations may be improved using the effect of particle-hole interactions. Unfortunately, shell-model calculations for Tb^{159} using the particle-hole interaction do not exist. Figure 4 shows structure at 10.1 MeV in the $Tb^{159}(\gamma,n)$ cross section which was also observed by Bogdankevich *et al.*[30] It should be possible to reproduce such structure with detailed shell-model calculations.

The semiclassical-hydrodynamic model[12] can be used[3,4,31] to explain the observed structure in the giant resonance. This theory predicts that the giant resonance for spheroidal nuclei is split into two Lorentz shaped components, whose peak cross sections occur at energies approximately inversely proportional to the lengths of the semimajor and semiminor axes. For prolate deformations (positive quadrupole moments) the area of the high-energy Lorentz component should be twice that of the lower energy component. Using this restriction, the sum of two Lorentz curves of the form

$$\sigma=\sigma_a/[1+(E^2-E_a^2)^2/\Gamma^2E^2]$$

has been fitted to the Tb^{159} formation cross section using an analog computor. The best fit obtained is shown as a solid curve in Fig. 5. The fit is in good agreement with the experiment up to 19 MeV. It was not possible to fit the experimental data with area restrictions corresponding to oblate deformation of the nucleus. The sum of the two Lorentz curves is considerably less than the data above 19 MeV. This effect cannot be explained by a simple direct interaction process, since the cross section above 19 MeV is due principally to $(\gamma,2n)$ reactions, which are not expected from fast interactions.

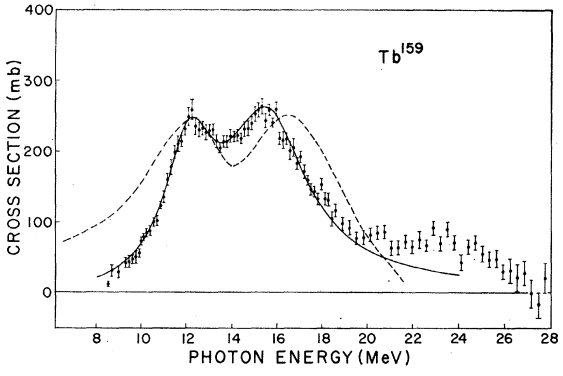

FIG. 5. The photon absorption cross section of Tb^{159} obtained by adding the (γ,n) and $(\gamma,2n)$ cross sections of Fig. 4. The electric dipole giant resonance is double peaked due to the quadrupole moment of Tb^{159}. The solid curve is the sum of two Lorentz curves with parameters given in Table III. The dashed curve is from Wilkinson (Ref. 9).

[24] B. G. Chidley, L. Katz, and S. Kowalski, Can. J. Phys. **36**, 407 (1958).
[25] H. B. Levy, Phys. Rev. **106**, 1265 (1957).
[26] J. M. Blatt and V. F. Weisskopf, *Theoretical Nuclear Physics* (John Wiley & Sons, Inc., New York, 1952), p. 379.
[27] T. Ericson, Advan. Phys. **9**, 425 (1960).
[28] A. G. Cameron, Can. J. Phys. **36**, 1040 (1950).
[29] E. V. Weinstock and J. Halpern, Phys. Rev. **94**, 1651 (1954).
[30] O. V. Bogdankevich, B. I. Goryachev, and V. A. Zaperalov, Zh. Eksperim. i Teor. Fiz. **42**, 1502 (1962) [English transl.: Soviet Phys.—JETP **15**, 1044 (1962)].
[31] E. G. Fuller and M. S. Weiss, Phys. Rev. **112**, 560 (1958).

The parameters of the fit shown in Fig. 5 are compared with those obtained in bremsstrahlung experiments[30–32] in Table III. Although the peak cross sections are in poor agreement, the peak energies and widths are in fair agreement. Note that Bogdankevich *et al.*[30] have obtained for Tb(γ,n) a ratio of areas of the two Lorentz components of 1.3 instead of 2.0 as predicted by hydrodynamic theory. They also suggest that their data are best explained by three widely spaced components corresponding to an asymmetric nucleus. A three Lorentz curve fit was made to our data. The quality of the fit was not improved by the additional parameters, since the sum of the two higher energy components was equal at all energies to the higher energy component of the two Lorentz curve fit. The present data do not determine whether Tb^{159} is prolately deformed or asymmetrically deformed, but they do rule out interpretation as three widely spaced components as suggested by Bogdankevich *et al.*[30] In all of the bremsstrahlung experiments of Table III an estimated correction for the $Tb^{159}(\gamma,2n)$ cross section was made, which is somewhat different from our measured $(\gamma,2n)$ cross section. The effect of using the measured $(\gamma,2n)$ cross section is to lower E_b by about 0.5 MeV. Even accounting for the $(\gamma,2n)$ effect, the difference in the bremsstrahlung cross section scale and our cross section scale is not simply a constant factor. We observe progressively lower cross sections than obtained in bremsstrahlung experiments as the photon energy is increased.

TABLE III. Parameters of the Tb^{159} giant resonance.

Parameter \ Reference	This experiment	Fuller and Weiss[a]	Thies and Spicer[b]	Bogdankevich *et al.*[c]
E_a (MeV)	12.2 ± 0.2	12.5	12.4±0.2	12.5
σ_a (mb)	188 ±19	260	410	267
Γ_a (MeV)	2.67± 0.2	2.4	3.3	3.4
E_b (MeV)	15.6 ± 0.2	16.3	16.0±0.2	16.4
σ_b (mb)	233 ±23	310	460	317
Γ_b (MeV)	4.30± 0.4	4.0	4.5	3.4
Q_0 (b)	+7.0 ± 1.1	7.7	7.3	7.8
$\int_8^{28}\sigma_t dE$ (MeV b)	2.3 ± 0.2			

[a] See Ref. 31.
[b] See Ref. 32.
[c] See Ref. 30.

The intrinsic quadrupole moment of Tb^{159} may be calculated[12] from the ratio of the peak energies of the Lorentz components; the only additional datum needed is a value for the mean nuclear radius. To facilitate a consistent comparison of the data, we present in Table III the intrinsic quadrupole moments calculated with a mean radius of (1.25 ± 0.06) $A^{1/3}$ F.[33] Our value for Q_0 is $+7.0\pm1.1$ b, and the agreement between the four experiments is good. The intrinsic quadrupole moment of the ground state of Tb^{159} may be calculated from the $B(E2)$ value for Coulomb excitation of the first rotational level. Sharp and Buechner[34] obtained $B(E2)=(3.6\pm0.6)\times10^{-48}e^2$-cm^4 which implies $Q_0=8.4\pm0.7$ b. The agreement between the Coulomb excitation value of Q_0 for the ground state and the value obtained in this experiment indicates that the quadrupole moment is not a strong function of excitation energy, since the transition energies depend upon some average quadrupole moment between the ground state and the excited state determined by the gamma-ray energy.

The photon absorption cross section of Tb^{159} is in good agreement with sum rule calculations. The Thomas-Reiche-Kuhn sum rule,[35] uncorrected for exchange effects, predicts that the integrated dipole absorption is $0.06NZ/A=2.31$ MeV-b, whereas the value obtained in this experiment, integrated from neutron threshold to 28 MeV, is 2.3 ± 0.2 MeV-b. The experimental integrated cross section should be further increased to account for dipole absorption below the neutron threshold and above 28 MeV, and decreased to account for transitions other than $E1$ transitions. An approximate way to perform this correction is to use the integrated cross section of the Lorentz curve fits to the data, which is 2.4 ± 0.2 MeV-b. The Migdal sum rule[35] is $\int\sigma(E)E^{-2}dE=2.25$ $A^{5/3}$ mb/MeV$=10.5$ mb/MeV, which agrees well with 10 ± 1 mb/MeV, our experimental result.

V. SUMMARY

Many features of the experimental photon cross sections of Tb and O are described by photonuclear theory in its present state, but the agreement between theory and experiment is not always quantitative. The identification of the numerous levels observed in O is incomplete. The widths and strengths of the resonances are not determined adequately by either experiment or theory, and we have no information on the spin and parity of the levels. The Tb integrated cross section is well described by $E1$ sum rules, and the intrinsic quadrupole moment obtained using the hydrodynamic model is in agreement with the ground-state quadrupole moment obtained by Coulomb excitation. The structure in the Tb cross section at 10.1 MeV and the high-energy tail of the cross section are not understood in detail. It would be desirable to have shell-model calculations including the particle-hole interaction for deformed nuclei such as Tb.

[32] H. H. Thies and B. M. Spicer, Australian J. Phys. **13**, 505 (1960).
[33] By analogy with the data on Ta^{181} of R. Hofstadter, Rev. Mod. Phys. **28**, 214 (1956).
[34] R. D. Sharp and W. W. Buechner, Phys. Rev. **109**, 1698 (1958).
[35] J. S. Levinger, *Nuclear Photo-Disintegration* (Oxford University Press, New York, 1960).